Syst Parasitol (2014) 89:175–183
DOI 10.1007/s11230-014-9519-y

A new species of *Glugea* Thélohan, 1891 in the red sea bream *Pagrus major* (Temminck & Schlegel) (Teleostei: Sparidae) from China

Youlu Su · Juan Feng · Xiuxiu Sun · Jingzhe Jiang · Zhixun Guo · Lingtong Ye · Liwen Xu

Received: 30 June 2014 / Accepted: 13 August 2014

Abstract A new microsporidian species is described from farmed red sea bream *Pagrus major* (Temminck & Schlegel) (Teleostei: Sparidae). Large numbers of spherical whitish xenomas were observed throughout the visceral organs of the host. Histological examination showed that the microsporidia caused several xenomas that were embedded in the intestinal muscularis externa or submucosa. Light and transmission electron microscopy examination of the spores also revealed morphological features typical of species of *Glugea* Thélohan, 1891. This microsporidian parasite has two different types of mature spores: microspores and macrospores. The spores are elongate-ovoid, with a large posterior vacuole. The polaroplast is bi-partite, with anterior and posterior parts comprising densely packed lamellae and loose membranes, respectively, and occupies approximately the anterior half of the spore. The polar filament is anisofilar, with 12–13 coils in a single layer almost touching the posterior spore wall. Comparison of the small subunit rDNA sequences revealed 92.7–98.1% identity with the sequences available from other *Glugea* spp. from piscine hosts. Phylogenetic analysis demonstrated that the microsporidian species studied clustered within the *Glugea* clade with strong support. Based on the differences in the morphological characteristics and molecular data, the microsporidian infecting *P. major* is considered to represent a species new to science, *Glugea pagri* n. sp.

Y. Su · J. Feng · J. Jiang · L. Ye · L. Xu (✉)
Key Laboratory of South China Sea Fishery Resources Exploitation & Utilization, Ministry of Agriculture, South China Sea Fisheries Research Institute, Chinese Academy of Fishery Sciences, Guangzhou 510300, Guangdong, China
e-mail: xuliwen@scsfri.ac.cn

X. Sun
Guangdong Provincial Aquatic Animal Epidemic Disease Prevention and Control Center, Guangzhou 510222, Guangdong, China

Z. Guo
Key Laboratory of Aquatic Product Processing, Ministry of Agriculture, South China Sea Fisheries Research Institute, Chinese Academy of Fishery Sciences, Guangzhou 510300, Guangdong, China

Introduction

The phyla Microsporidia and Cryptomycota, and the class Aphelidea have recently been considered to be a deep branch of the Holomycota lineage forming the so-called ARM (Aphelidea + *Rozella* + Microsporidia)-clade which is sister to the fungi (Karpov et al., 2014). The Microsporidia represent 1,300 to 1,500 species belonging to 187 genera. Of these, approximately 20 genera have been identified as teleost pathogens (Stentiford et al., 2013). These parasites produce chronic infections in host populations, increasing the morbidity and mortality rates in valuable fish species, such as salmonids (Rodriguez-Tovar et al., 2004), cod

(Brown et al., 2010) and also ornamental fish, including zebra fish (Ramsay et al., 2009). They are typically recognised by the formation of xenomas in the visceral organs or other vascularised tissues. The xenoma is a complex cyst-like structure comprising a hypertrophic host cell harbouring microsporidia in multiple stages of development (Matos et al., 2003; Lom & Dyková, 2005) and has a dual purpose: it not only protects the parasite from the host immune response but also confines the parasite in one site, preventing its dissemination throughout host body (Sprague & Hussey, 1980). Xenomas and spores can occlude blood vessels, causing a severe inflammatory response or death (Hauck, 1984). Microsporidia are of interest because they can be transmitted vertically or horizontally depending on species-specific microsporidium-host interactions (Sanders et al., 2013).

The red sea bream *Pagrus major* (Temminck & Schlegel) (Sparidae) is one of several important aquaculture species off the southern coast of China. In 2011, dying juvenile red sea bream were collected from a local fish farm in the Gulf of Daya, Guangdong Province, China in which large numbers of xenomas were observed throughout the visceral organs. Wet-mount preparations of the ruptured xenomas showed the presence of a microsporidian parasite, which likely belongs to the genus *Glug*ea Thélohan, 1891. The infection was associated with an approximately 50% mortality of the fish stock, leading to severe economic losses to the aquaculture industry. *Glugea* spp. similar to other microsporidia, cause substantial losses of teleost fishes in marine and freshwater habitats e.g. *Glugea stephani* Hagenmüller, 1899 in winter flounder *Pleuronectes americanus* (Walbaum) (see Khan, 2004) and *Glugea hertwigi* Weissenberg, 1911 in smelt *Osmerus eperlanus* L. (see Pekcan-Hekim et al., 2005). Although at least 17 species of *Glugea* infecting fish have been described, some of these species might be synonymous because their classification is based mainly on the host of origin and the morphology of the microsporidia (see Vagelli et al., 2005). Over past two decades, small subunit ribosomal DNA (SSU rDNA) sequence comparison has been a recognised technique for providing valuable information about phylogenetic relations. Thus, many studies on microsporidia are now including both morphological and comparative rDNA sequence characters (Lovy et al., 2009; Morsy et al., 2012). The current study represents a case report on infections in *P. major*, and provides a pathological, morphological and molecular characterisation of a new microsporidian parasite.

Materials and methods

Microscopic examination and histology

Juvenile *P. major* were reared in net pens (3 × 3 × 2 m) in seawater under natural conditions (salinity 29–30‰; temperature 24–26°C) in a fish farm at the Gulf of Daya, Guangdong, China. Fish were fed with trash fish twice a day. Samples of *P. major* were collected during the period of May to June 2011, anesthetised using MS-222 (Sigma-Aldrich) and measured (mean length 4.2 cm, range 3.5–6.0 cm) and weighed (mean weight 5.1 g, range 3.9–7.3 g). The diseased fish showed increased xenomas located throughout the visceral organs. The prevalence of infection was 54% (27 fishes out of 50 examined). Xenomas were removed and crushed in standard physiological saline under a coverslip, to release the spores. For morphological evaluation, spore smears were taken, examined by brightfield with a Leica DC 350F microscope (Leica, Germany) under a magnification of ×1,000 (oil immersion). Spore smears were fixed in absolute methanol and stained with phosphate-buffered Giemsa (pH 6.8). Arbitrarily selected, but undistorted, well-stained spores were measured using this optic microscope equipped with a specific software (Leica LAS). Visceral organs of infected fish were prepared for histology following standard fixation in 10% neutral buffered formalin and processing into paraffin wax blocks. Sections, 5 µm thick, were cut from blocks containing xenomas, processed and stained with haematoxylin and eosin. Stained sections were examined by brightfield, and images were captured digitally and measured by image analysis. All measurements are in micrometres unless otherwise indicated and are presented as the range followed by the mean in parentheses.

Transmission electron microscopy

For transmission electron microscopy (TEM), xenomas were fixed in 2.5% glutaraldehyde in 0.1 M phosphate buffer (pH 7.2) at 4°C for 24 h, rinsed overnight in the same buffer at 4°C, and postfixed in 2% OsO4 in the same buffer at 4°C for 4 h. After dehydration in an ascending ethanol series (70%, 80%, 90%, 95% and 100%; 2 h at each stage) and in propylene oxide (two changes for 3 h each), the

xenomas were infiltrated with Epon: propylene oxide solutions in the following ratios for 12 h in each solution: 1:1, 3:1, with a final infiltration in pure Epon. Ultrathin sections (30–40 nm) were cut on Reichert-Jung Ultracut E (Leica, Milton, Keynes, UK), stained for 1.5 h in 5% (w/v) aqueous uranyl acetate solution, then stained with lead citrate and examined with a Zeiss 902A TEM.

Molecular data

Xenomas were isolated from the visceral organs of the infected fish and preserved in 95% ethanol for DNA extraction, then ruptured by homogenisation procedure and spore suspensions were pipetted and centrifuged for 10 min at 5,000 *g*. The supernatant was discarded, and the spore pellet was dissolved in 50 µl STE buffer [10 mM Tris-HCl (pH 8), 100 mM NaCl, 0.25 mM EDTA, 0.5% SDS, and 0.4 mg/ml proteinase K]. Total genomic DNA was extracted from spores using a Universal Genomic DNA Extraction Kit (Takara, Japan) according to the manufacturer's protocol. The concentration of total genomic DNA was measured on a NanoDrop spectrophotometer (Thermo, USA) and the DNA samples were stored at −20°C until use. Based on SSU rDNA sequences for species of microsporidia in GenBank [accession numbers as follows: *Endoreticulatus* sp. (JN792450); *Pleistophora* sp. (D85500); *Glugoides intestinalis* Chatton, 1907 (AF394525); *Microsporidium* sp. (FJ794862)], the primers s1 (forward: 5′-ATG AGA CGT GAG AAA GAG TGC TTG GTA AA-3′) and a1 (reverse: 5′-CGC CGA CCG CAA CCT TGT TAC GAC TT-3′) were designed to amplify partial SSU rDNA sequences of the microsporidian parasite. Polymerase chain reaction (PCR) amplifications were performed in a 50 µl PCR reaction mixture containing 20 pmol of each primer, 2.5 U of Ex Taq polymerase (Takara, Japan) and 50 ng of genomic DNA. The reaction was run for 30 cycles at 95°C for 30 s, 55°C for 35 s, and 72°C for 2 min with a pre-denaturation step at 95°C for 5 min and a final extension step at 72°C for 10 min. The PCR products were separated and purified with a QiaexII Gel Extraction Kit (Qiagen, Germany), ligated with PMD18-T vector (Takara, Japan), transformed into *Escherichia coli* TOP10 (Invitrogen, USA), and sequenced.

To evaluate the relation of the present species with other known microsporidian species, a homology search was done using the BLAST program (http://www.ncbi.nlm.nih.gov/blast/). The SSU rDNA sequences for 25 microsporidian species available from the GenBank database (accession numbers listed in Fig. 4) were aligned together with the newly-generated sequence; *Beauveria bassiana* Bassi, 1835 (accession no. AF455504) was chosen as the outgroup. The sequences were aligned using Clustal W program (http://www.ebi.ac.uk/Tools/msa/clustalo/). The resulting alignment was checked and corrected manually using BioEdit (Hall, 1999). Neighbour-joining (NJ) analysis was performed with MEGA 6.0 (Tamura et al., 2013), using Kimura's two-parameter model and pairwise deletion of gaps. The confidence estimate in the NJ trees was obtained based on the bootstrap generation of 1,000 replicates.

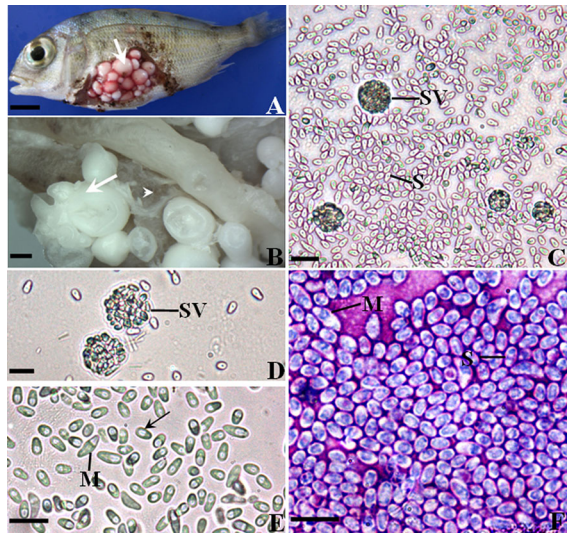

Fig. 1 Photographs of *Glugea pagri* n. sp. infecting *Pagrus major*. A, Large numbers of whitish xenomas (arrow) throughout the visceral organs; B, Some whitish xenomas (arrow) attached to the intestinal tract (arrowhead; formalin-fixed fish); C, Fresh spores of *G. pagri* after rupture of xenomas (fresh preparation; note that some sporophorous vesicles were not crushed); D, Sporophorous vesicles containing many mature spores (fresh preparation); E, Fresh mature spores, including a few macrospores, showing posterior vacuoles (arrows); F, Fixed spores, including a few macrospores, stained with Giemsa and showing spore body and darkly stained blue polar filament coil region. *Abbreviations*: MS, macrospores; S, spore; SV, sporophorous vesicles. *Scale-bars*: A, 0.5 cm; B, 0.1 cm; C–F, 10 µm

Results

Twenty-seven out of 50 fish examined (54.0%) were infected with microsporidian parasites. The diseased

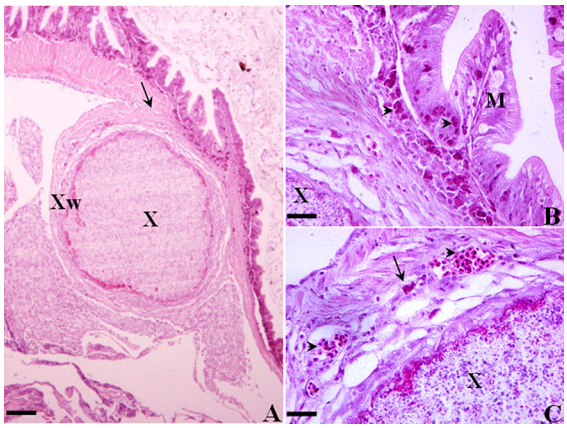

Fig. 2 Histopathology of *Glugea pagri* n. sp. infecting *Pagrus major*. A, Xenoma replacing and enlarging the normal muscularis externa (arrow) within the host intestine; B, Infiltration of eosinophilic granule cells (arrowheads) in the intestinal submucosa of infected fish; C, Inflammatory reaction in muscularis externa characterised by the presence of haemocyte aggregation in blood vessels (arrowheads) accompanied by infiltration of eosinophilic granule cells (arrow). *Abbreviations*: M, mucous cells; X, xenoma; Xw, xenoma wall. *Scale-bars*: A, 100 μm; B–C, 25 μm

fish showed lethargy and loss of appetite. Severely infected fish ceased eating and this was usually followed by death. Large numbers of spherical whitish xenomas were macroscopically observed attached to the visceral organs of most of the specimens (Fig. 1A, B). The infection developed as cyst-like masses up to 2 mm in diameter inducing enormous hypertrophy (Fig. 1A). Histological observations showed that xenomas filled with spores of the parasite were encapsulated by a wall or fibrous layer produced by the host and were attached in a wide distribution to the serosa of internal organs (Fig. 2A). In some cases xenomas replaced and enlarged a large proportion of the intestinal muscularis externa or submucosa. Inflammatory reaction characterised by the presence of hemocyte aggregation in blood vessels and accompanied by infiltration of eosinophilic granule cells (EGC) was observed, especially in the lamina propria (Fig. 2B, C).

Family Glugeidae Thélohan, 1892
Genus *Glugea* Thélohan, 1891

Glugea pagri n. sp.

Type-host: Red sea bream *Pagrus major* (Temminck & Schlegel) (Teleostei: Sparidae).

Type-locality: The Gulf of Daya, Shenzhen, China (22°36′ N, 114°32′ E).

Site of infection: Throughout the visceral organs of infected fish.

Prevalence: 54% (27 out of 50 fish) during the period of May to June 2011.

Type-material: Deposited at the Key Laboratory of South China Sea Fishery Resources Exploitation and Utilization, Ministry of Agriculture, South China Sea Fisheries Research Institute, Chinese Academy of Fishery Science, Guangzhou, China (syntypes, No. 2011SZ003-5).

Etymology: The specific name is derived from the generic name of the host species.

Description (Figs. 1, 3)

[Based on wet-mounts of xenomas from 5 specimens; measurements in micrometres.] Large numbers of mature spores present within sporophorous vesicles after rupture of xenomas (Fig. 1C, D). Spores elongate-ovoid or ellipsoidal, with posterior vacuole reaching midpoint (Fig. 1E). Two spore types present (Fig. 1E, F): ovoid or slightly ovoid microspores, 3.9–5.1 (4.4 ± 0.4) long and 2.1–3.0 (2.5 ± 0.3) wide (91.6% of spores; n = 40) and elongate-oval macrospores, 7.2–9.0 (7.9) long and 2.3–3.8 (2.9) wide (8.4% of spores; n = 20).

[Based on 10 spores from TEM images; measurements in nanometres.] Wall of xenoma composed of amorphous material interspersed with collagenous fibres and elements of host cell (Fig. 3A). Spore wall thinner at anterior pole, 100–120 (112), with thin electron-dense exospore and thick electron-transparent endospore (Fig. 3B). Mature spores elongate-ovoid, with large posterior vacuole in oblique position close to posterior pole. Nucleus located in centre of spore, compressed in the shape of spindle (Fig. 3B, C). Anchoring disc mushroom-like, located in centre of anterior pole of spore, attaching to polar filament; widest sectioned disc 374–388 (380) in diameter. Polar filament close to anchoring disc, 217–225 (220) in diameter; anterior part proceeding backwards to spore centre; posterior part with 12–13 coils in a single layer, nearly contiguous with spore wall; filament with distinct sequence of layers, 90–100 (94) in diameter (Fig. 3B–H). Polaroplast occupies approximately anterior half of spore, comprises lamellar polaroplast

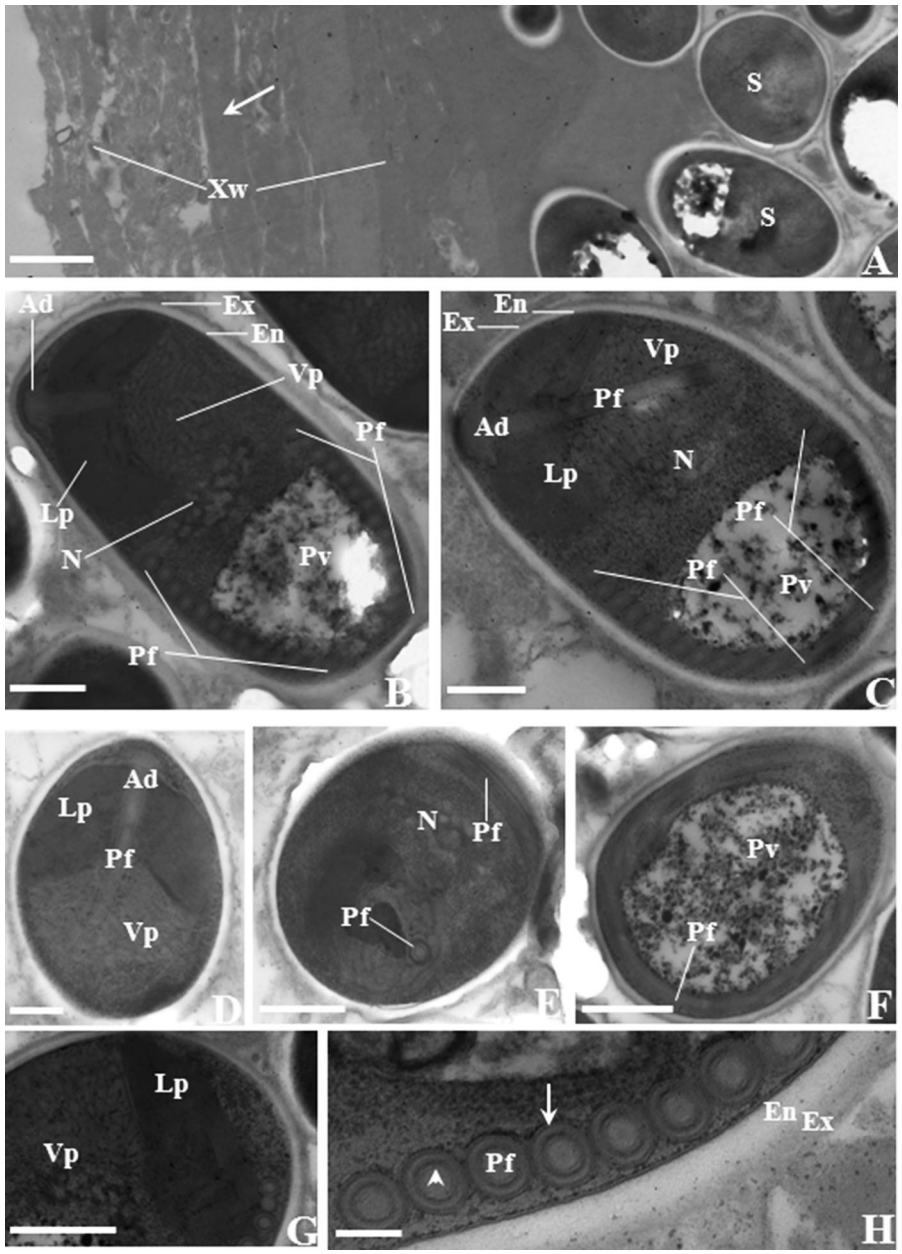

Fig. 3 Transmission electron micrographs of *Glugea pagri* n. sp. A, Xenoma wall covering mature spores composed of amorphous material interspersed with collagenous fibres (arrow); B, Longitudinal sections of a mature spore containing an anchoring disc, a single nucleus, a posterior vacuole and a polar filament with 13 coils; C, Longitudinal sections of a spore showing endospore, exospore, lamellar and vesicular polaroplasts, anchoring disk connected with the polar filament with 12 coils; D, Oblique section through a mature spore showing the anterior region with anchoring disk, polar filament, and lamellar and vesicular polaroplasts; E, Transverse section through a mature spore showing the nucleus and a cross section of the polar filament; F, Transverse section through mature spore showing the posterior region with posterior vacuole and a longitudinal section of the polar filament; G, Details of the polaroplast of a spore (note the lamellar polaroplast and the vesicular polaroplast); H, Details of polar filament coils showing the external membrane (arrow) and the concentric layers (arrowhead). *Abbreviations*: Ad, anchoring disc; En, endospore; Ex, exospore; Lp, lamellar polaroplast; N, nucleus; Pf, polar filament; Pv, posterior vacuole; S, spore; Vp, vesicular polaroplast; Xw, xenoma wall. *Scale-bars*: A, 1 μm; B–G, 0.5 μm; H, 100 nm

containing densely packed lamellae in anterior part and vesicular polaroplast with loose membranes extending posteriorly (Fig. 3C, D, G).

DNA sequencing and phylogenetic analyses

Sequencing of the partial SSU rDNA fragment from isolates of the new species produced a sequence of 964 bp, deposited in GenBank under accession number JX852026. BLAST search revealed that the parasite infecting *P. major* belongs to the genus *Glugea*, exhibiting the highest identity (98.1%) with *Glugea hertwigi*, *G. stephani* and *G. atherinae* Berrebi, 1979 and a high identity (> 92.7%) with other *Glugea* spp. from piscine hosts. There was a lower SSU rDNA sequence similarity (79.9–91.1%) with other microsporidian species mainly representatives of the genus *Pleistophora* Gurley, 1893 (Table 1). The distances observed between the novel sequence and those for other *Glugea* spp. were higher than 1.2% (Table 1). A phylogenetic analysis clearly demonstrated that *G. pagri* n. sp. clustered within the *Glugea* spp. clade containing *G. stephani*, *G. hertwigi*, *G. plecoglossi* Takahashi & Egusa, 1977, *G. atherinae*, *Glugea* sp. GS1 and *G. anomala* Moniez, 1887 (bootstrap support 92%; Fig. 4).

Discussion

Microsporidian infections represent a constant threat for aquaculture and the parasites are widely distributed in seawater, freshwater and estuaries (Kent & Speare, 2005). The present microsporidian parasite infecting netpen-reared *P. major* in seawater was recorded as whitish xenomas attached to the visceral organs of the host. As some microsporidia can easily be transmitted from fish to fish in the sea (Shaw et al., 1998), we speculate that sea water horizontal transmission of this parasite from wild marine fishes to netpen-reared *P. major*, is the possible source of the infection. The parasite also caused several xenomas in the host intestinal muscularis externa or submucosa accompanied by EGC infiltration. The presence of the xenomas in the submucosa is consistent with the findings reported by Lovy et al. (2009) for *G. hertwigi* and by Khan (2004) for *G. stephani.* EGC have been considered as fish mast cells and have been studied particularly in terms of their involvement in the fish immune response to parasites because they can produce serotonin and histamine (Reite, 1998). Similar tissue reactions have been described in the three-spined stickleback, *Gasterosteus aculeatus* L., infected with the microsporidian *G. anomala* (see Dezfuli et al., 2004).

In previous studies, microsporidia were mainly classified on the basis of their ultrastructural features, including the size and morphology of the spores, developmental stages in the life-cycle, and the number of coils of the polar filament (e.g. Larsson & Koie, 2005). A notable feature of *G. pagri* n. sp. is the presence of two morphologically different types of mature spores, the mean length of the larger spores being approximately 1.8-fold higher than the mean length of the smaller spores. Within the genus *Glugea*, the existence of species with two types of spores has been reported previously. For example, in *Glugea vincentiae* Vagelli, Paramá, Sanmartín & Leiro, 2005 infecting the Australian marine fish *Vincentia conspersa* (Klunzinger), microspores have a mean size of 5.1 × 2.2 μm and macrospores have a mean size of 8.9 × 3.1 μm (i.e. a 1.7-fold difference in mean length) (see Vagelli et al., 2005). The new species is similar to *G. vincentiae* in terms of the presence of two types of spores, but differs in terms of their smaller size, the slightly larger polaroplast (2.2 × 2.3 *vs* 1.7 × 2.0 μm), the single-layered polar filament, and the lack of stratified organisation typical of spores in mature xenomas. The number of coils in the polar filament is often diagnostic for microsporidian species in mature spores (Lovy et al., 2009). In this study, the number of coils of the polar filament inside the spore was 12–13, overlapping the range of 11–16 coils described for *G. anomala* and *G. stephani* (see Lom et al., 1995; Takvorian & Cali, 1996). *Glugea americanus* Takvorian & Cali, 1986, which had been transferred to the genus *Spraguea* Weissenberg, 1976, has polar filament with 6–8 coils i.e. out of the range of *Glugea* spp. (11–16 coils) (Keohane et al., 1996). Although *G. pagri* n. sp. shares most morphological similarities with *G. hertwigi*, especially the same number of coils and single-layered polar filament, it can be differentiated by the distinctly smaller nucleus (0.8 × 0.4 *vs* 1.4 × 0.7 μm) and the presence of two types of spores rather than one (see Lovy et al., 2009). This study represents the second observation of a microsporidian parasite infecting fishes of the genus *Pagrus* Cuvier. A comparison between the present

Table 1 Comparison of analysed SSU rDNA sequences: percentage of identity (above diagonal) and pairwise distance (below diagonal) obtained by Kimura's two-parameter analysis

	1	2	3	4	5	6	7	8	9	10	11	12	13	14	15	16	17	18
1. *Glugea pagri* n. sp.	–	98.1	98.1	98.1	97.9	97.7	92.7	91.1	90.5	90.2	90.0	89.5	89.2	88.9	88.4	86.9	82.7	79.9
2. *Glugea atherinae*	1.8	–	99.3	97.9	99.0	98.9	67.2	90.7	88.2	90.0	87.6	89.6	89.1	88.7	88.7	88.6	59.9	79.9
3. *Glugea hertwigi*	2.2	18.6	–	99.7	87.5	98.1	99.1	90.9	87.2	87.5	87.7	88.5	88.9	86.0	88.6	88.4	87.2	79.5
4. *Glugea stephani*	2.1	0.5	7.7	–	99.5	99.0	78.7	91.6	91.6	91.3	89.6	90.8	90.1	90.4	89.4	86.5	70.1	79.1
5. *Glugea plecoglossi*	2.2	0.8	16.5	0.4	–	86.7	76.1	90.8	87.3	87.1	87.5	88.6	88.5	77.4	88.3	88.2	70.6	80.3
6. *Glugea anomala*	2.5	12.0	9.6	1.6	11.7	–	98.3	90.2	86.1	86.6	87.4	87.8	88.1	85.4	87.7	88.1	86.6	79.9
7. *Glugea* sp. GS1	1.2	0.8	0.8	0.7	1.1	1.3	–	63.0	68.3	60.3	63.6	60.9	61.5	86.7	60.6	60.5	87.2	70.3
8. *Loma acerinae*	10.4	10.1	25.5	8.8	10.5	19.4	8.3	–	86.8	89.0	86.0	89.3	89.9	88.2	90.2	87.4	59.4	77.5
9. *Heterosporis anguillarum*	10.4	12.1	32.5	9.2	17.8	26.4	17.8	13.3	–	90.2	92.5	89.7	89.4	90.3	89.1	95.5	69.7	97.2
10. *Pleistophora ovariae*	10.5	11.2	27.0	9.6	11.4	20.2	8.8	12.5	7.3	–	98.1	92.0	90.9	88.8	90.9	94.2	59.9	90.0
11. *Pleistophora mirrandellae*	10.7	11.8	25.0	9.9	11.6	17.5	9.2	13.0	6.5	2.0	–	90.8	88.5	90.2	89.2	90.4	61.1	90.0
12. *Pleistophora hippoglossoideos*	12.0	11.5	27.3	10.2	11.8	20.7	10.8	12.2	8.8	8.7	9.0	–	92.4	98.3	91.9	91.5	60.7	86.7
13. *Trachipleistophora hominis*	12.2	11.9	27.5	10.7	12.1	21.0	10.3	12.1	10.2	10.5	11.0	8.1	–	91.2	96.2	90.6	59.5	82.7
14. *Pleistophora typicalis*	12.3	12.0	32.5	10.2	16.0	27.7	22.2	13.3	17.3	9.7	9.1	1.0	9.1	–	90.8	90.1	87.5	86.3
15. *Vavraia culicis*	12.9	12.5	28.3	11.3	12.4	21.4	11.2	11.8	10.2	10.3	10.7	8.9	3.9	9.6	–	90.4	59.4	81.9
16. *Heterosporis* sp. PF	10.5	12.2	27.5	9.8	12.6	20.2	9.0	13.6	3.0	7.4	6.9	9.3	10.3	9.5	10.7	–	58.0	96.0
17. *Microsporidium cypselurus*	11.0	10.5	13.9	10.1	12.0	14.7	14.0	12.5	20.2	12.0	11.9	10.9	12.6	19.5	12.9	12.2	–	56.6
18. *Pleistophora pagri*	23.0	22.4	22.0	23.5	21.9	21.5	17.5	24.2	2.5	7.6	7.6	11.3	14.2	11.4	15.2	3.7	28.2	–

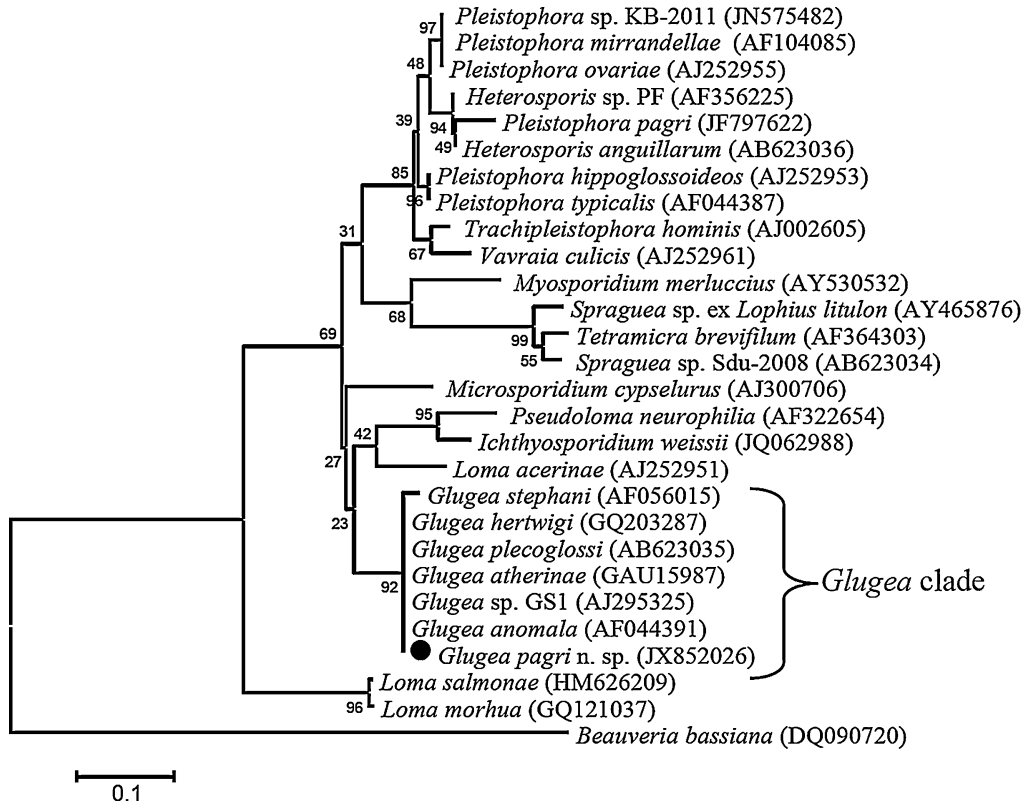

Fig. 4 Neighbor joining tree showing the relationships among *Glugea pagri* n. sp. infecting *Pagrus major* (black solid circle) and other microsporidians based on SSU rDNA sequences. The tree was generated using Kimura's two-parameter distance model using *Beauveria bassiana* as the outgroup. The scale-bar represents the number of substitutions per nucleotide site. Bootstrap support is based on 1,000 replicates. GenBank accession numbers are given in parentheses

species and *Pleistophora pagri* Morsy, Abdel-Ghaffar, Mehlhorn, Bashtar & Abdel-Gaber, 2012 described from *Pagrus pagrus* L. in Egypt by Morsy et al. (2012) reveals differences as follows. *Glugea pagri* n. sp. has larger spores (4.4 × 2.5 or 7.9 × 2.9 *vs* 1.7 × 1.5 μm) with long isofilar polar filament composed of a larger number of coils (12–13 *vs* 3–5). Moreover, the SSU rDNA data also clearly indicated that the new species is distinct from *P. pagri* (Table 1; Fig. 4).

SSU rDNA-based phylogenetic analyses have proven to be reliable criteria for assessing taxonomic relations among microsporidian species and are most suitable for the molecular characterisation of new species (Nath et al., 2012). The general structure of the phylogram in this study is consistent with previous analyses demonstrating that *Glugea* spp. form a distinct well-supported clade in the phylogenetic trees (Lovy et al., 2009; Abdel-Ghaffar et al., 2012). The high sequence identities and small distance values indicate a close relation between *G. pagri* n. sp. and other *Glugea* spp. for which DNA data are available to date (Table 1). Consequently, given the molecular data that provide strong resolving power for clade identification, we propose the designation of *Glugea pagri* n. sp. for the novel parasite infecting *P. major*, which also shares similar morphological characteristics within the *Glugea* group. Unfortunately, we were unable to describe the developmental stages of *G. pagri* n. sp. because xenomas contained only mature spores. This suggests that the parasite was no longer replicating in the xenomas examined. To clarify this, a TEM study on the morphological development of *G. pagri* n. sp. with emphasis on the merogonial and sporogonial stages should be conducted.

Acknowledgements This study was supported financially by Grants from the Special Scientific Research Funds for Central Non-profit Institutes, South China Sea Fisheries Research Institute, Chinese Academy of Fishery Sciences (codes 2012TS08, 2012A0503 and 2013A0604). We are grateful to

all the laboratory members for their technical advice and helpful discussions.

References

Abdel-Ghaffar, F., Bashtar, A. R., Morsy, K., Mehlhorn, H., Al Quraishy, S., Al-Rasheid, K., & Abdel-Gaber, R. (2012). Morphological and molecular biological characterization of *Pleistophora aegyptiaca* sp. nov. infecting the Red Sea fish *Saurida tumbil*. *Parasitology Research, 110*, 741–752.

Brown, A. M. V., Kent, M. L., & Adamson, M. L. (2010). Description of five new Loma (Microsporidia) species in Pacific fishes with redesignation of the type species *Loma morhua* Morrison & Sprague, 1981, based on morphological and molecular species-boundaries tests. *Journal of Eukaryotic Microbiology, 57*, 529–553.

Dezfuli, B. S., Giari, L., Simoni, E., Shinn, A. P., & Bosi, G. (2004). Immunohistochemistry, histopathology and ultrastructure of *Gasterosteus aculeatus* tissues infected with *Glugea anomala*. *Diseases of Aquatic Organisms, 58*, 193–202.

Hall, T. A. (1999). BioEdit: a user-friendly biological sequence alignment editor and analysis program for Windows 95/98/NT. *Nucleic Acids Symposium Series, 41*, 95–98.

Hauck, A. K. (1984). A mortality and associated tissue reactions of chinook salmon, *Oncorhynchus tshawytscha* (Walbaum), caused by the microsporidan *Loma* sp. *Journal of Fish Diseases, 7*, 217–229.

Karpov, S. A., Mamkaeva, M. A., Aleoshin, V. V., Nassonova, E., Lilje, O., & Gleason, F. H. (2014). Morphology, phylogeny, and ecology of the aphelids (Aphelidea, Opisthokonta) and proposal for the new superphylum Opisthosporidia. *Frontiers in Microbiology, 5*, 112.

Kent, M. L., & Speare, D. J. (2005). Review of the sequential development of *Loma salmonae* (Microsporidia) based on experimental infections of rainbow trout (*Oncorhynchus mykiss*) and Chinook salmon (*O. tshawytscha*). *Folia Parasitologica, 52*, 63–68.

Keohane, E. M., Takvorian, P. M., Cali, A., Tanowitz, H. B., Wittner, M., & Weiss, L. M. (1996). Identification of a microsporidian polar tube protein reactive monoclonal antibody. *Journal of Eukaryotic Microbiology, 43*, 26–31.

Khan, R. A. (2004). Effect, distribution, and prevalence of *Glugea stephani* (Microspora) in winter flounder (*Pleuronectes americanus*) living near two pulp and paper mills in Newfoundland. *Journal of Parasitology, 90*, 229–233.

Larsson, J. R., & Koie, M. (2005). Ultrastructual study and description of *Paramyxoides nephtys* gen. n., sp n. a parasite of *Nephtys caeca* (Fabricius, 1780) (Polychaeta: Nephtyidae). *Acta Protozoologica, 44*, 175–187.

Lom, J., & Dyková, I. (2005). Microsporidian xenomas in fish seen in wider perspective. *Folia Parasitologica, 52*, 69–81.

Lom, J., Noga, E. J., & Dyková, I. (1995). Occurrence of a microsporean with characteristics of *Glugea anomala* in ornamental fish of the family Cyprinodontidae. *Diseases of Aquatic Organisms, 21*, 239.

Lovy, J., Kostka, M., Dykova, I., Arsenault, G., Peckova, H., Wright, G. M., & Speare, D. J. (2009). Phylogeny and morphology of *Glugea hertwigi* from rainbow smelt *Osmerus mordax* found in Prince Edward Island, Canada. *Diseases of Aquatic Organisms, 86*, 235–243.

Matos, E., Corral, L., & Azevedo, C. (2003). Ultrastructural details of the xenoma of *Loma myrophis* (phylum Microsporidia) and extrusion of the polar tube during autoinfection. *Diseases of Aquatic Organisms, 54*, 203–207.

Morsy, K., Abdel-Ghaffar, F., Mehlhorn, H., Bashtar, A. R., & Abdel-Gaber, R. (2012). Ultrastructure and molecular phylogenetics of a new isolate of *Pleistophora pagri* sp. nov. (Microsporidia, Pleistophoridae) from *Pagrus pagrus* in Egypt. *Parasitology Research, 111*, 1587–1597.

Nath, B. S., Gupta, S. K., & Bajpai, A. K. (2012). Molecular characterization and phylogenetic relationships among microsporidian isolates infecting silkworm, *Bombyx mori* using small subunit rRNA (SSU-rRNA) gene sequence analysis. *Acta Parasitologica, 57*, 342–353.

Pekcan-Hekim, Z., Rahkonen, R., & Horppila, J. (2005). Occurrence of the parasite *Glugea hertwigi* in young-of-the-year smelt in Lake Tuusulanjärvi. *Journal of Fish Biology, 66*, 583–588.

Ramsay, J. M., Watral, V., Schreck, C. B., & Kent, M. L. (2009). *Pseudoloma neurophilia* infections in zebrafish *Danio rerio*: effects of stress on survival, growth, and reproduction. *Diseases of Aquatic Organisms, 88*, 69–84.

Reite, O. B. (1998). Mast cells/eosinophilic granule cells of teleostean fish: A review focusing on staining properties and functional responses. *Fish & Shellfish Immunology, 8*, 489–513.

Rodriguez-Tovar, L. E., Speare, D. J., Markham, R. J. F., & Daley, J. (2004). Predictive modelling of post-onset xenoma growth during microsporidial gill disease (*Loma salmonae*) of salmonids. *Journal of Comparative Pathology, 131*, 330–333.

Sanders, J. L., Watral, V., Clarkson, K., & Kent, M. L. (2013). Verification of intraovum transmission of a microsporidium of vertebrates: *Pseudoloma neurophilia* infecting the zebrafish, *Danio rerio*. *PLOS One, 8*, e76064.

Shaw, R. W., Kent, M. L., & Adamson, M. L. (1998). Modes of transmission of *Loma salmonae* (Microsporidia). *Diseases of Aquatic Organisms, 33*, 151–156.

Sprague, V., & Hussey, K. L. (1980). Observations on *Ichthyosporidium giganteum* (Microsporida) with particular reference to the host-parasite relations during merogony. *Journal of Eukaryotic Microbiology, 27*, 169–175.

Stentiford, G. D., Feist, S. W., Stone, D. M., Bateman, K. S., & Dunn, A. M. (2013). Microsporidia: Diverse, dynamic, and emergent pathogens in aquatic systems. *Trends in Parasitology, 29*, 567–578.

Takvorian, P. M., & Cali, A. (1996). Polar tube formation and nucleoside diphosphatase activity in the microsporidian, *Glugea stephani*. *Journal of Eukaryotic Microbiology, 43*, 102S–103S.

Tamura, K., Stecher, G., Peterson, D., Filipski, A., & Kumar, S. (2013). MEGA6: molecular evolutionary genetics analysis version 6.0. *Molecular Biology and Evolution, 30*, 2725–2729.

Vagelli, A., Paramá, A., Sanmartín, M. L., & Leiro, J. (2005). *Glugea vincentiae* n. sp. (Microsporidia: Glugeidae) infecting the Australian marine fish *Vincentia conspersa* (Teleostei: Apogonidae). *Journal of Parasitology, 91*, 152–157.